Vietnam Journal of Science and Technology ***63*** *(3) (2025) 502-516*

doi:10.15625/2525-2518/20164

Studies on electrical conductance and activation parameters of parchment supported lead molybdate model membrane

Mohd. Ayub Ansari[1, *], Dileep Kumar Singh[1], Haider Iqbal[1] , Manoj Kumar[2]

[1]*Department of Chemistry, Bipin Bihari College, Jhansi-284001, Uttar Pradesh, India*

[2]*Department of Chemistry, Hansraj College, University of Delhi, India*

[*]Email: *drayub67@gmail.com*

Received: 21 February 2024; Accepted for publication 16 August 2024

Abstract. The ion-interaction approach was used to develop a lead molybdate parchment supported model membrane. SEM, TEM, FT-IR, TGA, XRD, and EDX investigations were used to determine the physicochemical parameters. In order to understand the mechanism of transportation of ions , The absolute reaction rate theory has been utilized for diffusion processes in model membranes at temperature ranges between 10 °C and 50 °C, the electrical conductivity of a lead molybdate membrane supported on parchment was measured using different alkali chlorides. The sequence of the cations determines the electrical conductance values of the alkali chloride as $K^+ > Na^+ > Li^+$. The larger the positive hydrations of ions, the higher the activation energies follows the order $E_a\ K^+ > E_a\ Na^+ > E_a\ Li^+$. Crystallographic data suggest that bigger ions have a harder time penetrating the membrane than smaller ones. This explains why bigger ions must have larger thermodynamic activation parameters like E_a, $\Delta H^{\neq}$ and $\Delta G^{\neq}$ than smaller ions. Negative $\Delta S^{\neq}$ values show that ionic species are partially immobilized, most likely as a result of interstitial penetration and ionic interaction with the fixed charge group on the membrane skeleton.

Key words: Lead molybdate model membrane, Electrical conductance, Thermodynamic activation parameters.

Classification numbers: 2.5.2, 2.6.2, 2.10.3.

1. INTRODUCTION

Ion exchange membranes are selective barriers used in various fields such as wastewater treatment, food and juice industry, medical uses, energy, and gas sensing [1 - 4]. Vegetable parchment paper is a widely used material for fabricating membranes due to its gastric mucosal properties and excellent physical and chemical properties [5]. The electrochemical characterization of a parchment-supported membrane includes ion-exchange capacity, water content, nature, transport property, thickness, thermal and chemical stability, and structural properties [6]. These properties can be easily measured using various physical methods, as reported by various authors [7 - 10]. The electrochemical characterization of parchment-supported membranes is crucial for their applications in various fields [11]. Parchment supported

inorganic precipitate membranes (PSIPM) are frequently used as models for studying transport phenomena due to their stability in various environments.

This paper describes the fabrication of a lead molybdate membrane supported by parchment, which has been characterized using spectroscopic techniques such as SEM, TEM, XRD, and FT-IR. The study focuses on understanding the transport mechanism of ions and evaluating physicochemical parameters such as electrochemical characteristics and electrical conductance. The electrochemical characteristics and electrical conductance of the artificial membrane depend on the nature of the membrane-forming materials, the structure of the membrane, and the concentration and nature of the electrolyte solution [12, 13]. The absolute reaction rate theory has been used for diffusion processes in artificial membranes [14,15]. The membrane conductance was measured in contact with different concentrations of sodium chloride (NaCl), potassium chloride (KCl), and lithium chloride (LiCl) solutions at 10° to 50 °C. as these electrolytes have biological importance [16]. The fixed charge theory can provide a qualitative prediction of how specific conductance will vary depending on the concentration of the external solution [6, 17, 18]. Iijima *et al.* [19] used activation analysis namely free energy of activation, $\Delta G^{\neq}$, energy of activation, E_a, entropy of activation, $\Delta S^{\neq}$, and enthalpy of activation, $\Delta H^{\neq}$, of the membrane-electrolyte system, have been calculated at various temperatures, to study the mechanism governing the diffusivity of ions of simple salts via a membrane supported by parchment. The overall performance of a parchment-supported lead molybdate membrane depends on physical, chemical, and morphological transport features, as well as thermal and chemical mechanical stability.

2. MATERIALS AND METHODS

The model membrane was fabricated by using parchment paper supplied by Amol Group of Companies, Mumbai, India. Sodium molybdate (Na_2MoO_4) (S.D. Fine Limited, India), lead chloride $PbCl_2$ (Ranbaxy, India), and. For electrochemical characterization of membrane, the monovalent chlorides like lithium chloride (LiCl), potassium chloride (KCl) and sodium chloride (NaCl) were used. All the chemicals and reagents used were of analytical grade.

2.1. Membrane preparation

The ion-interaction approach proposed by Beg *et al.* [12, 20 - 22]. was used to construct the parchment-supported lead molybdate model membrane. After soaking for roughly 2 hours in deionized water, parchment paper was attached to the flat lip of a beaker containing a 0.2M sodium molybdate (Na_2MoO_4) solution. At room temperature, the beaker was suspended for 72 hours in a porcelain dish containing a 0.2M solution of lead chloride ($PbCl_2$). Later, the two solutions (the fresh solution) were swapped and stored for another 72 hours. On the surface of parchment paper. Fine deposition of lead molybdate was achieved in this manner. For the elimination of free electrolytes, the membrane was thoroughly rinsed with deionized water.

2.2. Electrical conductance measurement

The method suggested by Lakshminarayanaiah [23] was used to measure the membrane electrical conductance. As illustrated in Figure 1, the membrane was sandwiched between two pyrex glass half-cells. To equilibrate the membrane, the half cells were first filled with electrolyte solutions (KCl, NaCl, or LiCl). The solutions were replaced with pure Hg without the addition of the surface solvents. Any trapped air at the membrane-solution contact

was eliminated to get reproducible result. To determine electrical contacts, platinum electrodes were employed. At a frequency of 103 Hz, a direct digital conductivity meter 306 (Systronics, India) was used to measure the electrical membrane conductance. All measurements were taken at 10 °C, 20 °C, 30 °C, 40 °C, and 50 °C (± 0.1 °C).

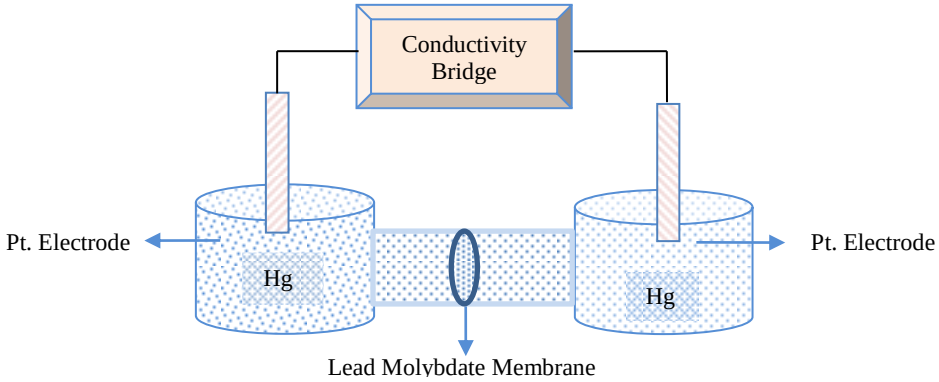

Figure. 1. Representation of cell assembly for electrical conductance measurement.

2.3. Characterization of the lead molybdate membrane

The electrochemical properties of the membrane are influenced by membrane parameters such as water uptake, porosity, thickness, swelling, etc., so it is required to characterize the complete membrane [24].

2.3.1. Water uptake percentage

The water uptake or percentage of water in membrane was determined as follows:

$$Water\ uptake\ (\%) = \left(\frac{W_w - W_d}{W_w} \right) x100 \quad (1)$$

where: W_w denotes the weight of the wet artificial membrane and W_d denotes the weight of the dry artificial membrane

2.3.2. Membrane porosity

The porosity (**Φ**) of membrane was calculated very easily through using the following equation:

$$Membrane\ \ Porosity = \left(\frac{W_w - W_d}{AL\,\rho_w} \right) \quad (2)$$

where ρ_w = density of water (g/cm^3), A = Area of membrane (cm^2), and L = thickness of membrane (cm).

2.3.3. Membrane thickness

Average thickness of the membrane was calculated by using screw gauze in order to detrermine the membrane thicknesss

2.3.4. Membrane swelling

The membrane swelling was determined as the difference in average thickness between the dry membrane and those that had been equilibrated in 1M sodium chloride solution for twenty-four hours.

2.3.5. Morphological and structural characterization

To check the membrane's microstructure, a SEM image was captured. The surface morphology was investigated by model JSM-7100F Oxford at an accelerating voltage of 15.0 kV. At 1 Pa of pressure, gold sputtered coatings were applied to the desired membrane sample.

In order to determine the particle size of lead molybdate membrane TEM analysis was done. The membrane TEM images were captured using a Thermo Scientific TM Talos L120C transmission electron microscope.

2.3.6. FT-IR analysis

The FT-IR spectrum of lead molybdate membrane was obtained using a Bruker Tensor 27 spectrophotometer from Germany. The scanning range was set to 4000 cm^{-1} to 800 cm^{-1}.

2*.3.7. Thermal characterization*

The thermal behavior and degradation process of the membrane were examined using a thermal analyzer Toledo-Mettler, United States, in a N_2 atmosphere at a heating rate of 20 °C per min from 25 °C to 600 °C.

2.3.8. XRD characterization

The X-ray diffraction (XRD) pattern of the membrane was produced using an X-ray diffractometer (Panalytical X' Pert Power) and Cu K radiations.

2.3.9 . EDX Analysis

The Energy Dispersive X-Ray (EDX) spectra of the lead molybdate membrane were obtained using a Scanning Electron Microscope (Model JSM-7100F Oxford).

3. RESULTS AND DISCUSSION

Table 1 shows the results of water uptake, porosity, thickness, and swelling of a parchment supported lead molybdate membrane.

Table 1. Water uptake, swelling, porosity, thickness, and properties of parchment supported lead molybdate model membrane.

Water uptake as % weight of wet membrane	1.097
Swelling (%)	0.98
Porosity (Φ)	0.0661
Thickness (mm)	1.059

A model membrane supported by parchment will absorb water based on the ambient vapour pressure. The high order of water absorption, porosity and swelling, with reduced membrane thickness shows that exchange sites are predominantly responsible for diffusion across the membrane [7, 25].

The SEM micrographs of the parchment-supported model membrane are presented in Figure 2 (a to b), and it is clear that surface morphology has a significant impact on membrane performance. Because the materials distribution, which is parchment paper and lead molybdate, was mixed consistently, the created membrane has a homogenous texture, which displays remarkable results and may be used for further study. Furthermore, heat treatment increases the compatibility of lead molybdate particles with binder parchment paper. The SEM image reveals that the surface of the parchment-based lead molybdate model membrane is flakes. The flakes would provide the metal ions with a 3-dimensional surface area for absorption. As a result, metal ion transport through this membrane would be impressive.

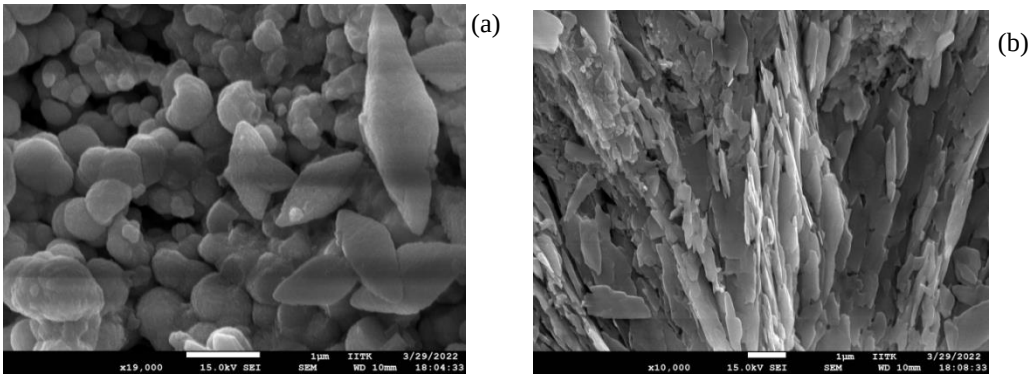

Figure 2. (a-b) Scanning electron microscopy of a lead molybdate membrane supported by parchment.

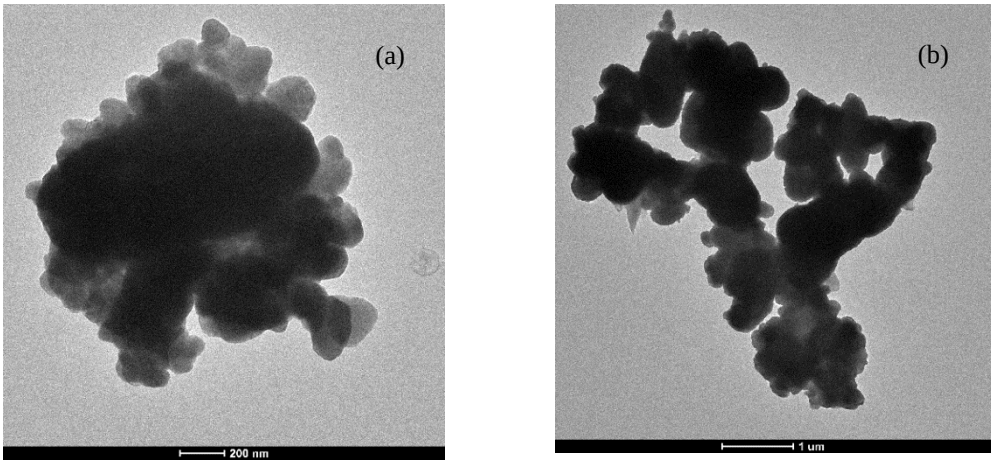

Figure 3. (a-b) Lead molybdate model membrane TEM micrographs.

Figure 3 shows TEM micrographs of the lead molybdate membrane. (a-b) on the surface of the parchment paper, the lead molybdate particles can be observed to be equally dispersed. The average particle size is close to 200 nm - 1 µm, which is somewhat bigger than the SEM determination. According to the TEM image, nanoparticles have a greater surface-to-volume ratio and just a tiny quantity of the substance is needed to fabricate the membrane.

The FT-IR spectra of lead molybdate membrane appeared in Figure 4. A low intensity peak formed in the range of 1496 cm^{-1} which indicates the C-H bond of vegetable parchment paper. The water peaks also found in the range of 3693 cm^{-1} to 3305 cm^{-1} but it appears to be very less intense. The sharp peak of water which stated that the lead molybdate material easily absorb the

water from the surrounding atmosphere. The spectra of supported lead molybdate material which clearly indicates the stretching modes of water and peaks found in the range of 1190 - 800 cm^{-1} respectively. The FT-IR study of the membrane also shows that the materials as the property of both constituents of membrane matrix. Others usual infrared bands were also observed at their appropriate position in the spectra. The peaks above 3700 - 3900 cm^{-1} show that overtones and combinations of bands of high-energy stretching vibrations of O-H bonds are present.

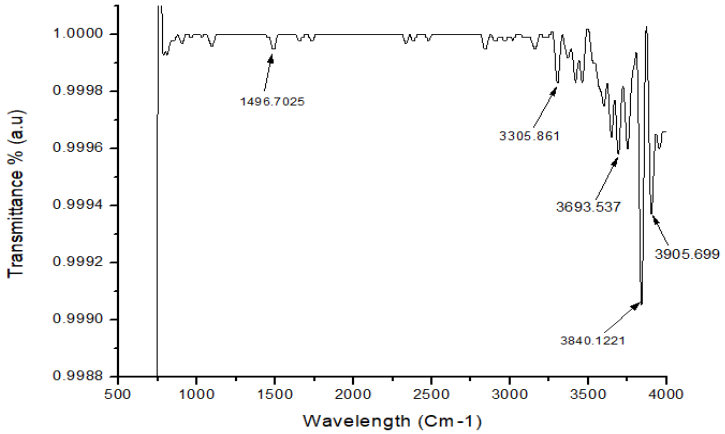

Figure 4. FT-IR spectra of lead molybdate model membrane.

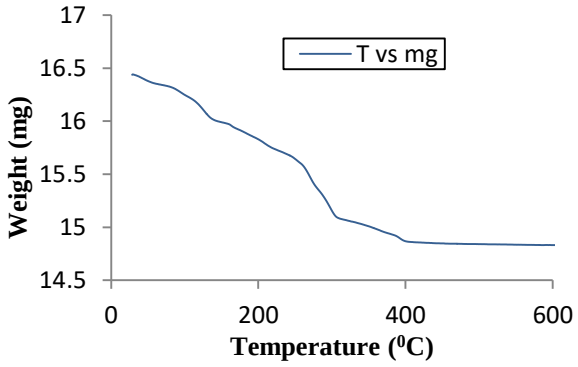

Figure 5. TGA curve of lead molybdate model membrane.

TGA was used to study thermal behavior of fabricated membrane under a N_2 atmosphere, as presented in Figure 5. The lead molybdate model membrane showed steady weight loss of about 15.99 mg and 15.58 mg between 147.2 °C and 260.0 °C, respectively, which may be attributed to the expulsion of external water molecules present at the surface of the materials. The second weight loss of the lead molybdate-based parchment supported membrane was 15.05 mg and 14.84 mg in temperature ranges of 326.0 °C and 464.6 °C, respectively, indicating the beginning of condensation as a result of the removal of lattice water from the material.

The XRD pattern of the parchment-supported membrane is depicted in Figure 6. The XRD pattern of the sample exhibited only one sharp diffraction peak centered at nearly 27.5°. According to JC-PDS Card No. 71-4970, the observed single peak was indexed at (112), and various less intense peaks are found from the 10 - 60° 2Θ values. The extremely sharp peak and various lesser peaks illustrate that the materials belong to distinct planes at different ranges.

Because of the existence of prominent peaks in the spectra, the membrane materials are utilized to form the membrane, which is highly crystalline.

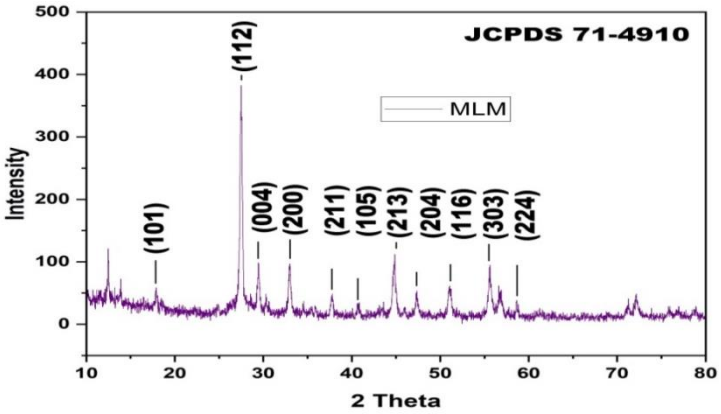

Figure 6. XRD pattern of lead molybdate model membrane.

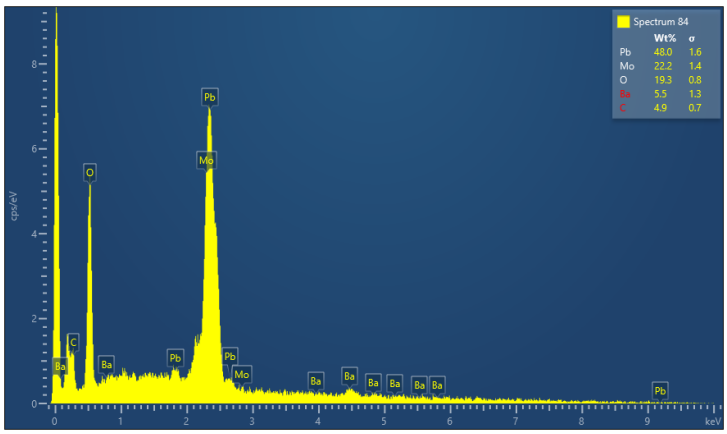

Figure 7. EDX spectrum of lead molybdate model membrane.

Table 2. Elemental composition of a membrane particle made up of lead molybdate.

Elements	% Weight	Atomic Wt.%
Mo	22.23	10.93
O	19.30	56.89
C	4.93	19.36
Pb	48.02	10.93
Ba	5.53	1.90

To validate the materials purity and composition, EDX analysis was done. Figure 7 displays the EDX spectrum of the membrane supported by parchment. From the EDX spectra, it has been determined that Table 2 contains only the pure forms of all the elements, such as C, O, Mo, and Pb, at the proper concentrations.

The electrical conductance of parchment supported lead molybdate membrane in contact with monovalent electrolytic (K^+Cl^-, Na^+Cl^- and Li^+Cl^-) solutions of various concentrations at 10 °C to 50 °C temperatures was measured repeatedly by performing experiment three times,

and its mean values along with the standard deviation are given in Tables (3 to 5) and plotted against the square root of the concentration ($C^{1/2}$). For the various solutions, these charts are shown in Figures 8 - 10. The membrane's electrical conductance values are positive and rise at all temperatures as the concentration of different electrolytic solutions does

Table 3. Electrical conductance ($m\Omega^{-1}cm^{-1}$) values measured experimentally for KCl electrolyte at various temperatures (10 °C to 50 °C) ± 0.1 °C

Electrolyte	Conc. (mol/l)	Temperature (℃)				
		10	20	30	40	50
KCl	0.1	10.25 ± 0.010	10.69 ± 0.015	11.68 ± 0.016	11.99 ± 0.016	12.78 ± 0.026
	0.5	6.62 ± 0.012	7.83 ± 0.015	8.56 ± 0.011	8.69 ± 0.015	9.62 ± 0.012
	0.05	5.58 ± 0.015	5.98 ± 0.016	6.75 ± 0.015	7.24 ± 0.015	7.69 ± 0.015
	0.02	4.70 ± 0.015	4.97 ± 0.019	5.12 ± 0.016	5.51 ± 0.012	5.82 ± 0.015
	0.01	3.15 ± 0.016	4.27 ± 0.015	4.62 ± 0.016	4.78 ± 0.015	5.12 ± 0.016

The values are expressed in mean ± standard deviation

Table 4. Electrical conductance ($m\Omega^{-1}cm^{-1}$) values measured experimentally for NaCl electrolyte at various temperatures (10 to 50) ± 0.1 °C.

Electrolyte	Conc. (mol/l)	Temperature (℃)				
		10	20	30	40	50
NaCl	0.1	9.98 ± 0.015	10.30 ± 0.010	10.62 ± 0.015	11.56 ± 0.011	12.26 ± 0.013
	0.5	5.59 ± 0.015	5.80 ± 0.016	6.62 ± 0.016	7.49 ± 0.016	8.85 ± 0.015
	0.05	4.70 ± 0.016	5.25 ± 0.015	6.95 ± 0.015	7.30 ± 0.019	7.82 ± 0.026
	0.02	3.92 ± 0.012	4.44 ± 0.019	5.86 ± 0.015	6.55 ± 0.015	6.90 ± 0.015
	0.01	3.88 ± 0.015	4.35 ± 0.015	5.25 ± 0.023	5.30 ± 0.016	5.86 ± 0.015

The value are expressed in mean ± standard deviation

Table 5. Electrical conductance ($m\Omega^{-1}cm^{-1}$) values measured experimentally for LiCl electrolyte at various temperatures (10 °C to 50 °C) ± 0.1 °C.

Electrolyte	Conc. (mol/l)	Temperature (℃)				
		10	20	30	40	50
LiCl	0.1	7.29 ± 0.016	7.82 ± 0.017	8.55 ± 0.016	9.29 ± 0.015	9.98 ± 0.015
	0.5	4.86 ± 0.016	5.29 ± 0.015	5.92 ± 0.016	6.19 ± 0.016	6.86 ± 0.015
	0.05	3.75 ± 0.015	4.28 ± 0.015	4.92 ± 0.016	5.80 ± 0.015	6.18 ± 0.019
	0.02	3.62 ± 0.019	3.85 ± 0.012	4.45 ± 0.022	4.85 ± 0.016	5.20 ± 0.020
	0.01	3.30 ± 0.010	3.65 ± 0.015	4.29 ± 0.019	4.48 ± 0.019	5.89 ± 0.015

The values are expressed in mean ± standard deviation.

According to Figures 8 to 10, the membranes' specific conductance increases with bathing electrolyte solution concentration and achieves a maximum limiting value at higher concentrations utilized at all temperatures. With respect to their conductance behavior at various electrolytic concentrations, these results are consistent with those obtained for synthetic membranes. The electrolytes specific conductance values correspond to the cations in the following order:

$$K^+ > Na^+ > Li^+$$

ion diffusion is also influenced by the membrane's charge and porosity. The above-mentioned order appears to be determined by the membrane's porosity and the size of the hydrated species

diffusing across the membrane. The size of the hydrated ions may be significantly influenced by a number of probable water molecule configurations under certain temperature conditions [26, 27].

In this method, the electrical conductance would rise with rising temperature, but only if the membrane's structure didn't suffer any irreversible changes. The linear plots of log π against 1/T displayed in Figure 11 demonstrate that there was no such structural change involved. According to the Arrhenius equation, the slope of this yields the energy of activation (E_a).

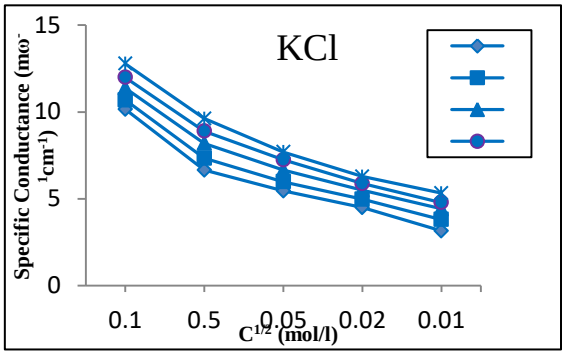

Figure 8. Plot of specific conductance vs $C^{1/2}$ for the KCl electrolyte across the lead molybdate membrane at various temperatures (10 °C to 50 °C).

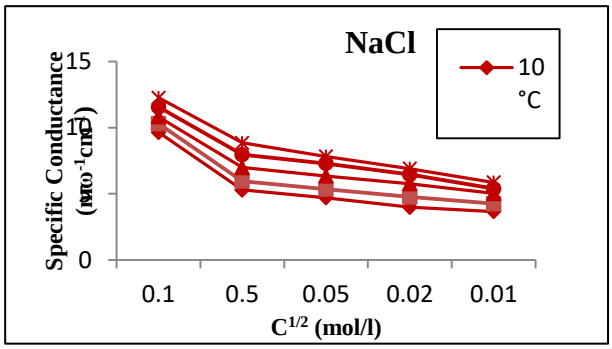

Figure 9. Plot of specific conductance vs $C^{1/2}$ for the NaCl electrolyte across the lead molybdate membrane at various temperatures (10 °C to 50 °C).

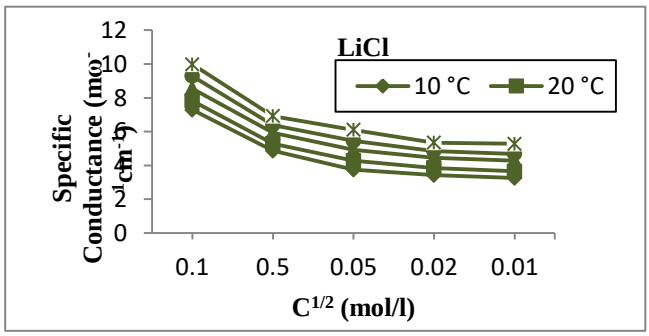

Figure 10. Plot of specific conductance vs $C^{1/2}$ for the LiCl electrolyte across the lead molybdate membrane at various temperatures (10 °C to 50 °C).

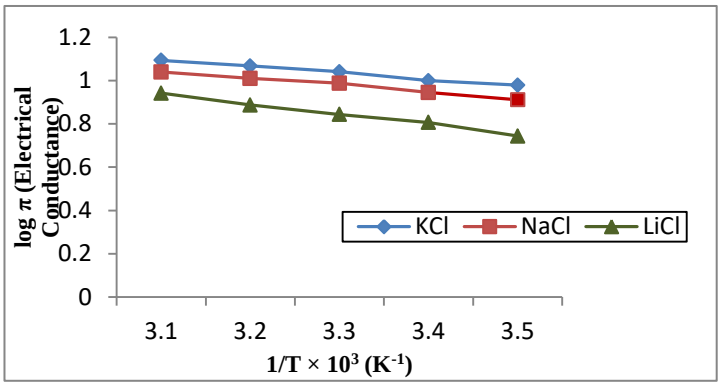

Figure 11. Arrhenius plots of electrical conductance against $1/T \times 10^3$ for different alkali chlorides across lead molybdate membrane.

Table 6 shows that the energy of activation decreases as the concentration of the bathing electrolytic solution increases, and the order of the energy is as follows:

$$Ea\ K^+ > Ea\ Na^+ > Ea\ Li^+$$

Table 6. Theoretical values of activation parameters for different alkali chlorides across lead molybdate membrane.

Electrolyte	**Conc.(mol/L)**	**E_a (KJ/mole)**	**$\Delta H^{\neq}$(KJ/mole)**	**$\Delta G^{\neq}$(KJ/mole)**	**$-\Delta S^{\neq}$($JK^{-1}mol^{-1}$)**
KCl	0.1	11.03	7.95	71.15	217.18
	0.01	12.95	11.30	78.18	231.32
NaCl	0.1	9.14	6.40	69.40	220.19
	0.01	12.97	11.12	78.15	233.25
LiCl	0.1	7.26	4.50	68.58	218.04
	0.01	12.31	10.12	77.24	235.07

Table 7. Comparision of calculated values of activation parameters for different alkali chlorides across lead molybdate membrane.

Electrolyte	**Conc (mol/L)**	**E_a (KJ/mole)**	**E_a (KJ/mole) Afren *et al.* [7]**	**$\Delta H^{\neq}$ (KJ/mole)**	**$\Delta H^{\neq}$ (KJ/mole) Afren *et al.* [7]**	**$\Delta G^{\neq}$ (KJ/mole)**	**$\Delta G^{\neq}$ (KJ/mole) Afren *et al* . [7]**	**$-\Delta S^{\neq}$ ($JK^{-1}mol^{-1}$)**	**$-\Delta S^{\neq}$ ($JK^{-1}mol^{1}$) Afren *et al.* [7]**
KCl	0.1	**11.03**	10.01	**7.95**	6.99	**71.15**	70.11	**217.18**	214.17
	0.01	**12.95**	11.99	**11.30**	10.22	**78.18**	77.16	**231.32**	229.30
NaCl	0.1	**9.14**	8.12	**6.40**	5.32	**69.40**	68.37	**220.19**	215.17
	0.01	**12.97**	11.99	**11.12**	10.01	**78.15**	77.12	**233.25**	230.22
LiCl	0.1	**7.26**	6.21	**4.50**	3.45	**68.58**	67.54	**218.04**	216.01
	0.01	**12.31**	11.33	**10.12**	9.03	**77.24**	76.23	**235.07**	231.04

From Table 7, we can conclude that the values of the calculated various activation parameters are in accordance with our previous work [7] and also in accordance with the findings of Beg *et al.* [13].

Data obtained from Table 8, is in the favour of the applicability of Kumins [28] effects for membrane systems supported on parchment is confirmed by a decline in activation energy with a decrease in crystallographic radius.

Table 8. Relationship between the activation energy of an electrolyte and its crystallographic radius.

Ion	Crystallographic radii (Å)	Energy of activation (KJ/mole)
K^+	1.56	10.98
Na^+	1.15	8.16
Li^+	1.06	6.97

According to Eyring [29], the membrane pores may be thought of as a series of energy barriers that the particle must leap over to get through them throughout the transportation process.

According to absolute reaction rate theory [29].

$$\kappa = \left(\frac{RT}{Nh}\right) e^{-\left(\frac{\Delta H^{\neq}}{RT}\right)} e^{\left(\frac{\Delta S^{\neq}}{R}\right)} \tag{3}$$

where κ = Experimental electrical conductance, R = Universal gas constant, T = Absolute temperature, N = Avogadro number, h = Planck's constant, $\Delta H^{\neq}$ = Enthalpy of activation and $\Delta S^{\neq}$ = entropy of activation respectively.

The $\Delta H^{\neq}$ and $\Delta S^{\neq}$ are determined by the Gibbs-Helmholtz equation.

$$\Delta G^{\neq} = \Delta H^{\neq} - T\Delta S^{\neq} \tag{4}$$

$\Delta H^{\neq}$ is determined with the help of activation energy E_a, as

$$E_a = \Delta H^{\neq} + RT \tag{5}$$

As shown in Figure. 12, the membrane conductance values were calculated and plotted against $\log \frac{\kappa N h}{RT}$ and 1/T. RT gives the value of $\Delta H^{\neq}/R, \Delta S^{\neq}/R$ and E_a were calculated by using equations (4) and (5). Table 6 lists the various thermodynamic activation parameter values, including Ea, $\Delta H^{\neq}$, $\Delta G^{\neq}$, and $\Delta S^{\neq}$, as they were calculated for the diffusion of various alkali chlorides in membrane. According to the data, the ions tend to permeate at a negative value of $\Delta S^{\neq}$. The sequence of $\Delta S^{\neq}$ among the cations is as follows:

$$K^+ > Na^+ > Li^+$$

The relative partial immobility increased with an increase in the valence of cations, establishing the alkali chloride, and the $-\Delta S^{\neq}$ showed diffusion with partial immobilization in the inorganic precipitated membrane. [30]

According to Eyring [29], the values of $\Delta S^{\neq}$ represent the flow mechanism; a high positive value of $\Delta S^{\neq}$ is thought to reflect bonds breaking, whereas a low value denotes penetration without bonds breaking. Negative $\Delta S^{\neq}$ values are thought to either show that the permeating species and the membrane material have formed a covalent bond or that the permeation through the membrane may not really be the rate-determining process.

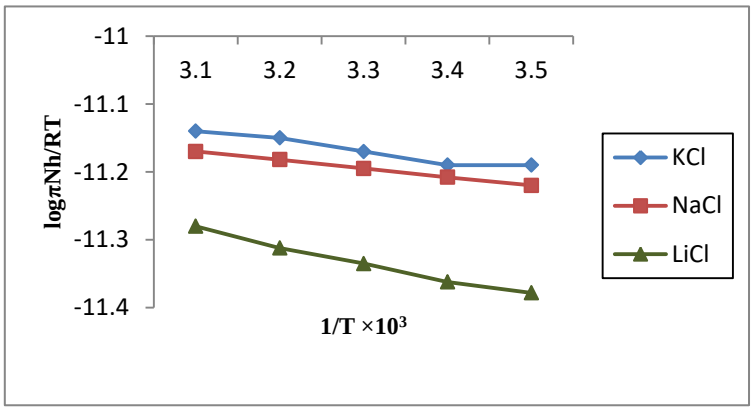

Figure 12. Plots of logπNh/RT Vs 1/T 10^3 for 1:1 alkali chloride through lead molybdate membrane

Barrer [28, 31] established the idea of "zone activation" and applied it to gas permeation via synthetic membranes. The zone activation theory suggests that a high $\Delta S^{\neq}$ value correlates with high energy of activation for diffusion, indicating either a broad zone of activation or reversible loosening of membrane chain segments. A low $\Delta S^{\neq}$ value indicates a narrow zone of activation or no loosening of the membrane during penetration. Conversely, Tien and Ting [32], who discovered negative $\Delta S^{\neq}$ values for water permeation through a very thin (50 A° thickness) bilayer membrane, emphasized the potential for the solution-membrane interface-rather than the membrane-to be the permeation rate-determining step. The interaction between the ions and the membrane fixed charge groups, resulting in partial immobilization, attributed the reason for negative $\Delta S^{\neq}$ values.

Overall, these studies show that it is possible to reasonably accurately calculate membrane conductivity at various temperatures. The ionic species flowing across the membrane pores maintain, to some extent, their hydration shell due to the weak charge of the membrane. Ionic interaction with fixed charge groups on the membrane skeleton and interstitial penetration might be the causes of the partial immobilization of ions indicated by negative $\Delta S^{\neq}$ values.

4. FUTURE IMPLICATIONS

PSIPM research offers numerous opportunities for innovation by integrating knowledge from materials science, chemistry, environmental science, and engineering. The key challenge is to transition from lab models to practical, real-world applications and create market-ready products. PSIPMs, used in water purification and industrial catalysis, offer hope for driving progress and addressing global issues through practical applications.

5. CONCLUSION

At temperature ranges between 10°C and 50°C, the electrical conductivity of a lead molybdate membrane supported on parchment was measured using different alkali chlorides. The sequence of the cations determines the electrical conductance values of the alkali chloride as K^+> Na^+> Li^+. Crystallographic data suggest that bigger ions have a harder time penetrating the membrane than smaller ones. This explains why bigger ions must have larger thermodynamic activation parameters like E_a, $\Delta H^{\neq}$, and $\Delta G^{\neq}$ than smaller ions. Negative $\Delta S^{\neq}$ values show that

ionic species are partially immobilized, most likely because of interstitial penetration and ionic interaction with the fixed charge group on the membrane skeleton.

Acknowledgements We express our gratitude to the Government of Uttar Pradesh for the financial assistance under the research and development scheme (No. 70/2021) and Principal, Bipin Bihari, College, Jhansi (U.P.) for providing the necessary facilities. We are also thankful for the Director, IIT Kanpur (U.P.) for FT-IR, TGA, SEM, XRD and Elemental analysis, AIIMS, Delhi for TEM analysis.

Author Contributions. Mohd Ayub Ansari**:** Supervision; Conceptualization, Data analysis; Dileep Kumar Singh: Experimental design; Methodology. Haider Iqbal: Experimental design, Data Curation; Writing & Manuscript editing; Manoj Kumar: Visualization, formal analysis.

Conflicts of Interest. The authors declare that they have no known competing financial interests or personal relationships that could have appeared to influence the work reported in this paper.

REFERENCES

1. Nasim Beg M., Siddiqi F. A., Shyam R., Altaf I. - Studies with inorganic precipitate membranes: Part XXVI. Evaluation of membrane selectivity from electric potential and conductivity measurements, J. Electroanal Chem. Interfacial Electrochem **98** (2) (1979) 231-240. https://doi.org/10.1016/S0022-0728(79)80263-6.
2. Singh K. P., Dobhal R., Prajapati R. K., Kumar S., Sanjesh, Ansarid M. A. - Preparation of isoproturon and 2,4-dichlorophenoxy acetic acid imprinted membranes: Ion transport study, Desalin Water Treat. **24** (1 - 3) (2010) 176-189. https://doi.org/10.5004/DWT. 2010.1497.
3. Thanh Hoai Ta Q., Ngoc Tri N., Noh J. S. - Improved NO2 gas sensing performance of 2D MoS2/Ti3C2Tx MXene nanocomposite, Appl. Surf. Sci. **604** (2022) 154624. https://doi.org/10.1016/J.APSUSC.2022.154624.
4. Prajapati R. K., Ansari M. A., Iqbal H. - Sustainable Municipal Solid Waste Management through Membrane Science and Technology, Waste Recover. Manag. an Approach Towar. Sustain. Dev. Goals (2023) 323-342. https://doi.org/10.1201/9781003359784-18.
5. Teorell T. - Studies on the "Diffusion Effect" upon Ionic Distribution, Some Theoretical Considerations, Proc. Natl. Acad. Sci. **21** (3) (1935) 152-161. https://doi.org/10.1073/ PNAS.21.3.152.
6. Zehra A., Khan M. M. A. - Rafiuddin - Modified composite cation exchange membrane with enhanced stability and electrochemical performance, J. Solid State Electrochem **25** (2) (2021) 489-504. https://doi.org/10.1007/S10008-020-04821-W/TABLES/3.
7. Ansari A., Shukla A. K., Ansari M. A. - Preparation, characterization and electrical conductance studies of inorganic precipitate parchment supported barium molybdate membrane, Mater. Today Proc. **47** (2021) 1445-1451. https://doi.org/10.1016/ J.MATPR.2021.03.302.
8. Arsalan M., Rafiuddin - Fabrication, characterization, transportation of ions and antibacterial potential of polystyrene based Cu3 (PO4)2/Ni3 (PO4)2 composite membrane, J. Ind. Eng. Chem. **20** (5) (2014) 3568-3577. https://doi.org/10.1016/ j.jiec.2013.12.050.
9. Arsalan M., Zehra A., Khan M. M. A., Rafiuddin - Preparation and characterization of polyvinyl chloride based nickel phosphate ion selective membrane and its application for

removal of ions through water bodies, Groundw. Sustain. Dev. **8** (2019) 41-48. https://doi.org/10.1016/j.gsd.2018.06.008.

10. Ishrat U., Dar A. M., Rafiuddin - Synthesis, characterization and electrochemical properties of cation selective ion exchange composite membranes, Arab. J. Chem. **12** (4) (2019) 580-587. https://doi.org/10.1016/J.ARABJC.2014.08.023.
11. Elsherif K. M., Yaghi M. M. - Studies with Model Membrane: The Effect of Temperature on Membrane Potential, Moroccan J. Chem. **5** (1) (2017) J. Chem. 5 N°1 (2017) 131-138. https://doi.org/10.48317/IMIST.PRSM/MORJCHEM-V5I1.6324.
12. Nasim Beg M., Siddiqi F. A., Singh S. P., Prakash P., Gupta V. - Studies with inorganic precipitate membrane: evolution of thermodynamically effective fixed charge density and test of the most recently developed theory of membrane potential based on the principles of non-equilibrium thermodynamics, Electrochim. Acta **24** (1) (1979) 85-88. https://doi.org/10.1016/0013-4686(79)80046-8.
13. Beg M. N., Ahmad K., Altaf I., Arshad M. - Ionic transport of alkali chlorides in parchment supported cupric orthophosphate membrane and application of absolute reaction rate theory, J. Memb. Sci. **9** (3) (1981) 303-311. https://doi.org/10.1016/S0376-7388(00)80271-9.
14. Zwolinski B. J., Eyring H., Reese C. E. - Diffusion and membrane permeability. I, J. Phys. Colloid Chem. **53** (9) (1949) 1426-1453. https://doi.org/10.1021/J150474A012.
15. Brooke N. M., Rees L. V. C. - Kinetics of ion exchange. Part 1, Trans. Faraday Soc. **64** (0) (1968) 3383-3392. https://doi.org/10.1039/TF9686403383.
16. I S., S B. - Electrolytes, Pharmacol. Vet. Anesth. Analg. (2019) 362-369. https://doi.org/10.1002/9781118975169.ch29.
17. Bahru J., Syarifah M., Syakiylla N., *et al*. - Poly (Ether Ether Ketone) Based Anion Exchange Membrane for Solid Alkaline Fuel Cell: A Review, J. Membr. Sci. Res. **5** (3) (2019) 205-215. https://doi.org/10.22079/JMSR.2018.86969.1194.
18. Kim J. F. - Recent Progress on Improving the Sustainability of Membrane Fabrication, J. Membr. Sci. Res. **6** (3) (2020) 241-250. https://doi.org/10.22079/JMSR.2019.106501.1260.
19. Iijima T., Obara T., Isshiki M., Seki T., Adachi K. - Ionic transport of alkali chlorides in nylon membrane, J. Colloid Interface Sci. **63** (3) (1978) 421-425. https://doi.org/10.1016/S0021-9797(78)80003-4.
20. Beg M. N., Siddiqi F. A., Shyam R. - Studies with inorganic precipitate membranes: Part XIV. Evaluation of effective fixed charge densities, Can. J. Chem. **55** (10) (1977) 1680-1686. https://doi.org/10.1139/v77-237.
21. Beg M. N., Siddiqi F. A., Shyam R., Altaf I. - Studies with inorganic precipitative membranes. XI. Membrane potential response, characterization and evaluation of effective fixed charge density, J. Electroanal. Chem. **89** (1) (1978) 141-147. https://doi.org/10.1016/S0022-0728(78)80039-4.
22. Beg M. N., Matin M. A. - Studies with nickel phosphate membranes: Evaluation of charge density and test of recently developed theory of membrane potential, J. Memb. Sci. **196** (1) (2002) 95-102. https://doi.org/10.1016/S0376-7388(01)00582-8.
23. Lakshminarayanaiah N. - Transport phenomena in membranes. https://cir.nii.ac.jp/crid/1130282272797504384Accessed12 February 2024.
24. Arsalan M., Rafiuddin - Fabrication, characterization, transportation of ions and

antibacterial potential of polystyrene based Cu3 (PO4)2/Ni3 (PO4)2 composite membrane, J. Ind. Eng. Chem. **20** (5) (2014) 3568-3577. https://doi.org/10.1016/J.JIEC.2013.12.050.

25. Ansari A., Shukla A. K., Ansari M. A. - Potentiometric determination of fixed charge density and antibacterial activity of barium molybdate model membrane, Malaysian J. Chem. **23** (3) (2021) 92-107. https://ksascholar.dri.sa/en/publications/potentiometric-determination-of-fixed-charge-density-and-antibactAccessed12 February 2024.
26. Nichka V. S., Mareev S. A., Apel P. Y., Sabbatovskiy K. G., Sobolev V. D., Nikonenko V. V. - Modeling the Conductivity and Diffusion Permeability of a Track-Etched Membrane Taking into Account a Loose Layer, Membr. 2022, Vol. 12, Page 1283 **12** (12) (2022) 1283. https://doi.org/10.3390/MEMBRANES12121283.
27. Bondarenko M., Yaroshchuk A. - Computational Design of an Electro-Membrane Microfluidic-Diode System, Membr. **13** (2) (2023) 243. https://doi.org/10.3390/MEMBRANES13020243.
28. Kumins C. A. - Transport through polymer films, J. Polym. Sci. Part C Polym. Symp. **10** (1) (1965) 1-9. https://doi.org/10.1002/POLC.5070100103.
29. Glasstone S., Laidler K. J. (Keith J., Eyring H. - The theory of rate processes : the kinetics of chemical reactions, viscosity, diffusion and electrochemical phenomena (1941). https://ci.nii.ac.jp/ncid/BA4327824XAccessed27 April 2025.
30. Shuler K. E., Dames C. A., Laidler K. J. - The Kinetics of Membrane Processes. III. The Diffusion of Various Non-Electrolytes through Collodion Membranes, J. Chem. Phys. **17** (10) (1949) 860-865. https://doi.org/10.1063/1.1747078.
31. Barrer R. M., Skirrow G. - Transport and equilibrium phenomena in gas–elastomer systems. I. Kinetic phenomena, J. Polym. Sci. **3** (4) (1948) 549-563. https://doi.org/10.1002/POL.1948.120030410.
32. Tien H. T., Hie Ping Ting - Permeation of water through bilayer lipid membranes, J. Colloid Interface Sci. **27** (4) (1968) 702-713. https://doi.org/10.1016/0021-9797(68)90104-5.